NUCL SCI TECH (2019) 30:93
https://doi.org/10.1007/s41365-019-0614-2

Design and commissioning of B_{rav} measurement system for SC200 superconducting cyclotron

Man-Man Xu[1] · Yun-Tao Song[2] · Gen Chen[2] · Yong-Hua Chen[2] · Kai-Zhong Ding[2] · Heng-Bo Li[3] · Jun Wang[3] · Jian Zhou[2]

Received: 28 March 2018 / Revised: 30 September 2018 / Accepted: 23 November 2018 / Published online: 15 May 2019

Abstract The SC200 proton therapy superconducting cyclotron was developed by ASIPP (Hefei, China) and JINR (Dubna, Russia). A measurement system was designed to assess the average radial component of the magnetic field (B_{rav}) with 15 search coils in the median plane. The winding differences of the search coils affect the measurement accuracy of the B_{rav}. Based on the electromagnetic induction principle, to measure the B_{rav} accurately, this paper focuses on the design and commissioning of the B_{rav} measurement system. The preliminary results confirm that the system design is reasonable and suitable. After testing the search coil at different speeds, the optimal speed was determined as 2.5 mm/s. The relative error was approximately 0.1% under the maximum radial component of the magnetic field B_r of 7 G. The measurement precision was up to 1.0×10^{-3}, which can provide the required measurement tolerance of 3–7 G for B_r in the median plane. The commissioning of the B_{rav} measurement system is an important step for B_r measurement. It can check and adjust the asymmetry of the superconducting coils (SCs).

Keywords Superconducting cyclotron · Magnetic field · Measurement system · Commissioning

This work was supported by the Natural Science Foundation of Anhui under Grant (No. 1908085QA25), the Research Initiation Foundation of Anhui Polytechnic University (No. 2018YQQ001), the Pre-Research National Natural Science Foundation of China of Anhui Polytechnic University (No. 2019yyzr13), the National Natural Science Foundation of China (Nos. 11575237 and 11775258), the National Magnetic Confinement Fusion Science Program (No. 2015GB101001), and the International Scientific and Technological Cooperation Project of Anhui (No. 1704e1002207).

✉ Gen Chen
chengen@ipp.ac.cn

1 School of Mechanical and Automotive Engineering, Anhui Polytechnic University, Wuhu 241000, China

2 Institute of Plasma Physics, Chinese Academy of Sciences, Hefei 230026, China

3 Hefei CAS Ion Medical and Technical Devices Co., Ltd, Hefei 230088, China

1 Introduction

The SC200 proton therapy superconducting cyclotron will be able to accelerate protons to an energy of 200 MeV with a maximum beam intensity of 1 μA. The average magnetic field of the cyclotron is up to 3.6 T [1, 2]. As a key component of the cyclotron, the superconducting magnet provides the isochronous magnetic field with a strong focusing force to restrict beam movement. However, the asymmetry of sectors and the superconducting coils (SCs) generates a radial component, B_r, of the magnetic field in the median plane, directly affecting the vertical deviation of the beam orbit from the median plane [3–6].

A number of measurement methods have been proposed to measure the average radial component of the magnetic field (B_{rav}), including nuclear magnetic resonance (NMR) [7], hall probes [8–10], and flux measurements with search coils [3, 11–14]. To design such a measurement system, the field strength, homogeneity, variation in time, and required accuracy should be considered. Search coils are highly sensitive and less strongly influenced by the vertical component of the magnetic field (B_z), which is more accurate than the hall probes for magnetic field measurement. The use of a variety of search coils is the most-often used tool for characterizing field qualities in cyclotrons [15–18].

For SC200, the B_{rav} measurement system was designed to measure the B_{rav} of the magnetic field by using search coils with a high testing accuracy. The B_{rav} measurement system mainly includes a drive system, control system, and data acquisition system. In particular, based on the electromagnetic induction principle, there are 15 search coils moving in the magnetic field to measure the B_{rav}. The minimum and maximum measurement radii were 30 mm and 620 mm, respectively. The search coils are made of copper and covered with an insulating varnish. Owing to the quality differences in the winding process, it is necessary to perform the commissioning of the search coil outside of the SC200 cyclotron.

In this study, we present a detailed design and investigate the required commissioning work to improve B_{rav} measurement accuracy. This paper describes the B_{rav} tolerance analysis, the commissioning platform design, and research. The analysis and results are of great significance for the B_{r} measurement of the SC200 proton therapy superconducting cyclotron.

2 B_{rav} tolerances for SC200 superconducting cyclotron

Owing to the asymmetry of sectors and SCs, the B_{rav} existing in the azimuth-varied field cyclotron, which causes the effective median plane (EMP) of the magnetic system, does not coincide with the median plane of the cyclotron. The EMP was formulated by Botman and Hagedorn for the cyclotron work region [3]. Thus, the tolerances for the B_{rav} of the magnetic field should be estimated.

When the magnetic system symmetry is broken, stable vertical oscillations exist near the EMP. The horizontal field component exists in the median plane. To separately identify the tolerances for the horizontal field components from the permitted vertical beam offset, the B_{rav} can be written as:

$$B_{\mathrm{rav}} = Z_{\mathrm{eff}} B_{\mathrm{zav}} Q_{\mathrm{z}}^{2}/R, \tag{1}$$

where Z_{eff} is the vertical position of the EMP, B_{zav} is the average vertical component of the magnetic field at radius R, Q_{z} represents the vertical betatron frequency, and R is the magnetic field radius.

The SC200 superconducting cyclotron has been proposed and designed [17, 19–21]. The isochronous field B_{zav} distribution is shown in Fig. 1a, and the maximum magnetic field was approximately 3.54 T [20, 22]. From the computed vertical betatron frequency Q_{z} in Fig. 1b, Eq. (1) shows the tolerance distribution of B_{rav} for the acceptable vertical offset of the beam of 1 mm shown in Fig. 2.

With the frequency Q_{z} close to 0.32 in the extraction region, the isochronous field B_{zav} was approximately 3.54 T. The B_{rav} tolerance in the median plane was approximately 3–7 G, as shown in Fig. 2. Consequently, the testing resolution of the B_{rav} measurement system should be smaller than 1 G.

3 Commissioning platform design

3.1 Testing principle

The magnetic flux distribution produced by the test coil had an excitation current of 2 A, as shown in Fig. 3. It generates a magnetic field of 3–7 G, the same as the magnetic field B_{rav} tolerance of SC200 superconducting cyclotron.

A commissioning diagram comprising a test coil and 15 concentric search coils is shown in Fig. 4. According to the electromagnetic induction principle, when the search coils move in the magnetic field, the induced voltage U is generated, which can be integrated by the fluxmeter. The testing flux change $\Delta\Phi_{\mathrm{t}}$ can be written as:

$$\Delta\Phi_{\mathrm{t}} = \int U \mathrm{d}t. \tag{2}$$

The radial component change ΔB_{r} can be calculated using:

$$\Delta B_{\mathrm{r}} = \Delta\Phi_{\mathrm{t}}/A. \tag{3}$$

The effective sensitive area of the search coil A is:

$$A = N \cdot 2\pi R \cdot 2\Delta Z. \tag{4}$$

where N is the number of search coil turns, R is the coil radius, and ΔZ is the distance shift from the median plane.

The search coil was first connected to the fluxmeter, which was shifted from its initial position of $-\Delta z$ to a terminal position of $+\Delta z$. The fluxmeter acquired the magnetic flux generated by the coil. Subsequently, the other coils were changed to connect to the fluxmeter, and the previous steps were repeated.

3.2 Platform design

Based on the testing principle, the search coils must be a priority during design. The search coils comprised copper wire, with a diameter of 0.3 mm, covered with insulating varnish. The search coils were numbered from C1 to C15. Each coil could be connected to the LINKJOIN LZ840 fluxmeter by a coil selector. Then, the coil parameters, including the radius, the number of turns, and the coil resistance, were sent to the fluxmeter. The distribution of the search coils on the disk is shown in Fig. 5.

The input coil parameters are shown in Table 1.

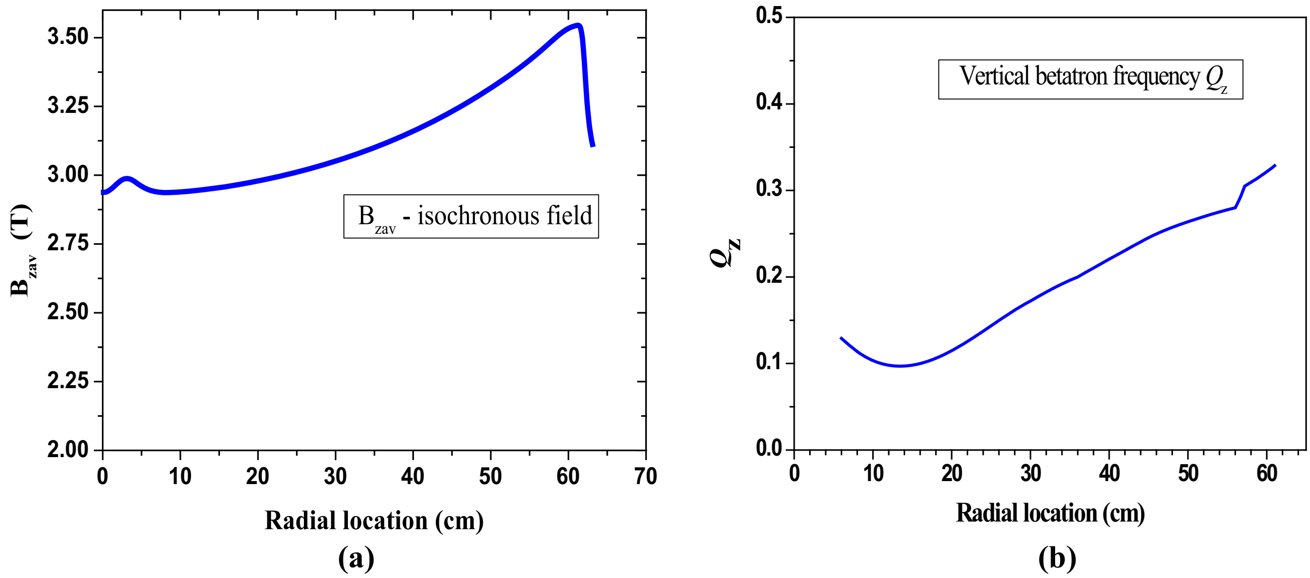

Fig. 1 **a** B_{zav} distribution along the radius for SC200 cyclotron and **b** vertical betatron frequency Q_z for SC200 cyclotron

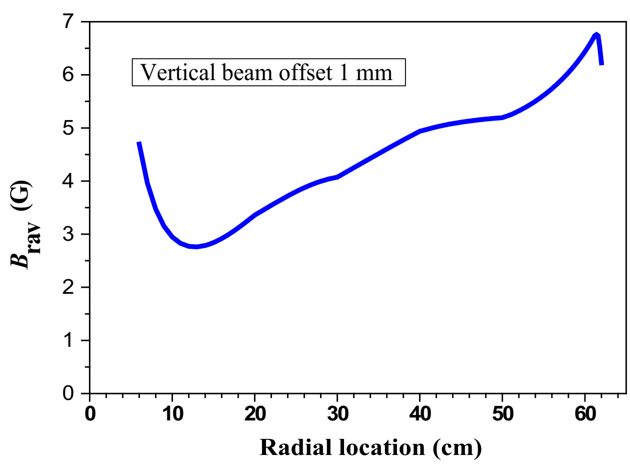

Fig. 2 B_{rav} for the acceptable vertical offset of the beam of 1 mm

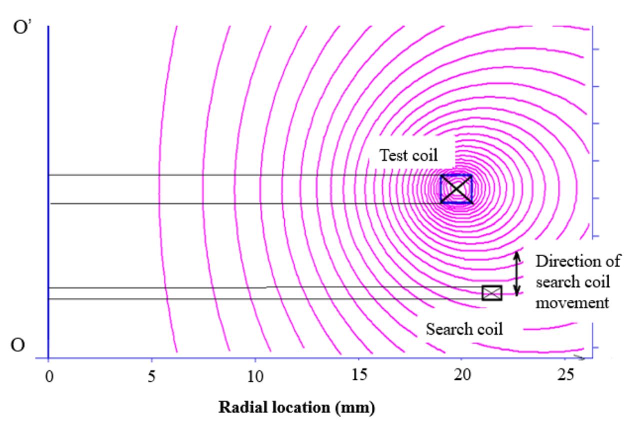

Fig. 3 (Color online) Magnetic flux distribution

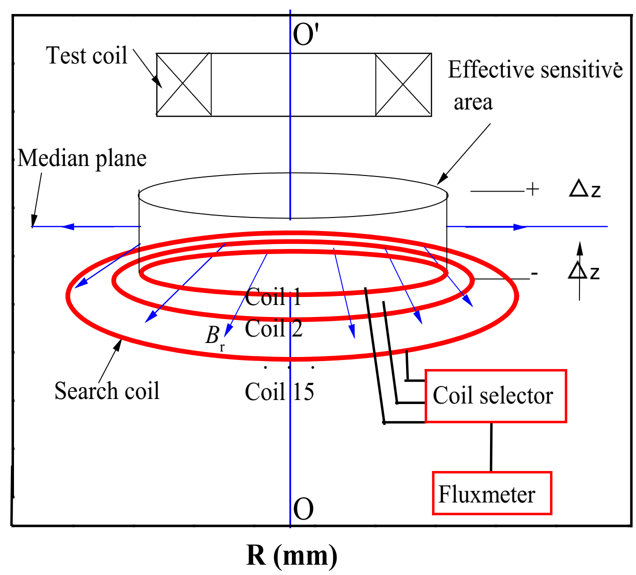

Fig. 4 (Color online) Testing diagram of the search coil

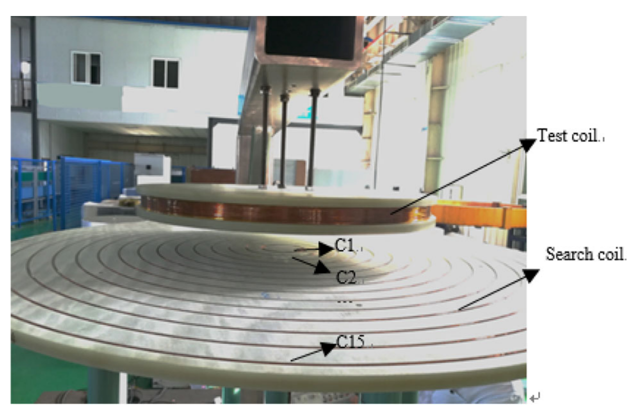

Fig. 5 (Color online) Distribution of search coils

Table 1 Search coil parameters

Coil no.	C1	C2	C3	C4	C5	C6	C7	C8	C9	C10	C11	C12	C13	C14	C15
Radius R (mm)	30	55	80	105	130	155	180	205	230	255	280	305	330	355	380
Number of turns N	34	26	20	16	10	10	8	8	8	6	6	6	6	6	6
Coil resistance (Ω)	7.705	7.822	8.038	7.847	7.914	8.15	8.051	8.236	8.547	7.91	8.108	8.237	8.53	8.622	8.855

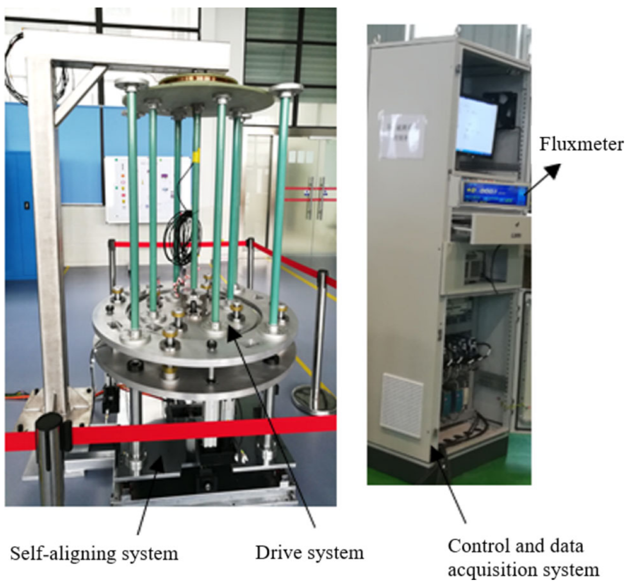

Fig. 6 (Color online) Commissioning platform

The commissioning platform of the B_{rav} measurement system was designed with a drive system, control system, and data acquisition system, as shown in Fig. 6. The self-aligning system includes two groups of cross screws and linear guide structures. These institutions can adjust the disk center coinciding with the geometric center of the superconducting cyclotron. The drive system can drive the search coils to move along the vertical axis of the cyclotron. The control system comprises the parameter settings area, the data and status display area, and the logic control area. The data acquisition system is responsible for collecting the measurement signals. The LINKJOIN LZ840 fluxmeter collects the flux signal with high sensitivity, which should be warmed for 5 min and done zero setting and drift setting before using.

To avoid the magnetic field influence from B_z, it is necessary to adjust and confirm the relative position between the test coil and search coil. An angular error of 1 mrad will produce an approximately tenfold error in the B_r value. Therefore, the parallelism of the search coil and test coil must be less than 0.4 mm, and that of the concentricity must be less than 0.5 mm. In this way, the B_r value will not be influenced by the B_z value.

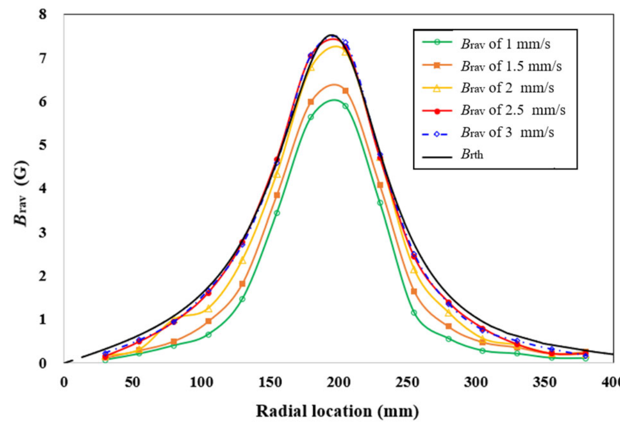

Fig. 7 (Color online) B_{rav} measurement results under different search coil speeds

4 Commissioning and discussion

To confirm that the B_{rav} measurement system operates well, based on the testing principle above, system commissioning should be conducted outside the cyclotron. The drive system made the search coils move from their initial position of − 10 mm to the terminal position of + 10 mm. The fluxmeter acquired the first flux $\Phi 1$ generated by the first search coil C1. Subsequently, the second flux $\Phi' 1$ was generated when the disk moved in reverse. Following this, C2 was switched to connect to the fluxmeter, and the previous steps were repeated. This was performed sequentially until coil C15, and all the measurement data were collected for further analysis.

We found that the coil speed affects the B_{rav} results. Thus, the testing was conducted with five different speeds in the range of ± 10 mm. The collected flux was fitted by the least-square method. The B_{rav} is calculated using Eq. 3 in Fig. 7, and the trend of the B_{rav} curves is consistent. The theoretical value (B_{rth}) was provided by the TOSCA software. The B_{rav} was closer to the B_{rth} as the coil speed increased from 1 to 2.5 mm/s. There were no obvious relative error changes between the 2.5 and 3 mm/s speeds.

Compared with B_{rth}, the relative error of B_{rav} was calculated and is shown in Fig. 8. The relative error of B_{rav} with a speed of 2.5 mm/s was the smallest. The relative error of the curves is greater in two edge radius ranges. When increasing the coil speed, the flux variation within a unit time will increase correspondingly. Thus, the signal-to-noise ratio will be promoted. For the fluxmeter, the disturbance caused by noise will comprise a smaller proportion and the measurement results will be more accurate at the points where the value of the signal-to-noise ratio is larger. Otherwise, owing to the structure parameters of the fluxmeter, the original right signal completely becomes the interfering signal. In the case of a severe signal drift, the effective signal is often submerged. Therefore, 2.5 mm/s is considered to be the optimal speed for the search coil.

Following this, the search coils were shifted four times with a speed of 2.5 mm/s. The B_{rav} distributions were deduced and are shown in Fig. 9. The B_{rth} and B_{rav} curves are consistent, as shown in Fig. 10. The B_{rav} denotes the average measured value from four B_{rav} values.

As shown in Fig. 11, the relative error curve first increases and then decreases with the increase in radius. The minimum error occurred at $R = 205$ mm, corresponding to C8. The minimum relative error was 0.09513% with a B_{rav} of 7 G, which continued to be increasing to approximately 12.37% for B_{rav} of 1 G at the edge point. In addition, the smallest absolute error and biggest absolute error of ΔB_{rav} were 0.006857 G and 0.05402 G, respectively, both less than 1 G.

The measurement accuracy of the B_{rav} changed with the radial location. For the radial range of 0–205 mm, the magnetic field intensity increased together with the measuring accuracy. For the radial range of 205–380 mm, the measuring accuracy decreased. There is a low intensity at both ends of the B_r distribution curve as the measurement accuracy is susceptible to interference. The measurement accuracy was high under the high-intensity field in the middle radial position.

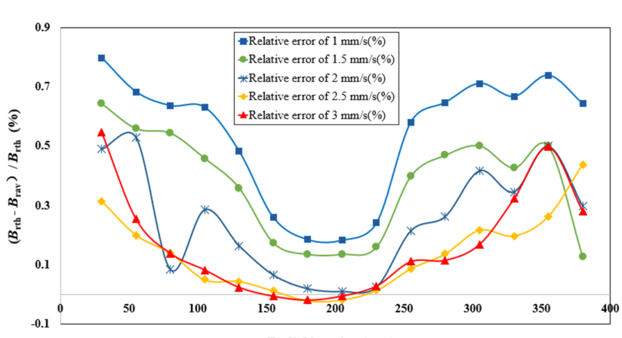

Fig. 8 (Color online) Relative error results under different search coil speeds

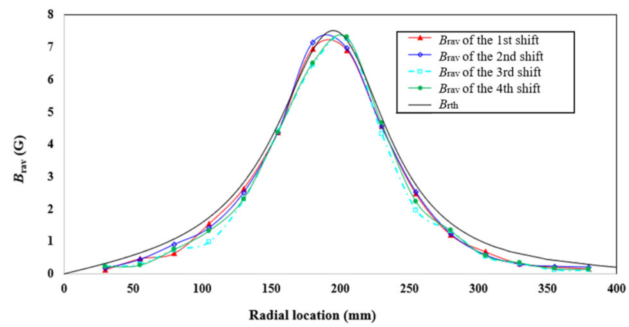

Fig. 9 (Color online) B_r measurement results with a vertical movement of ± 10 mm

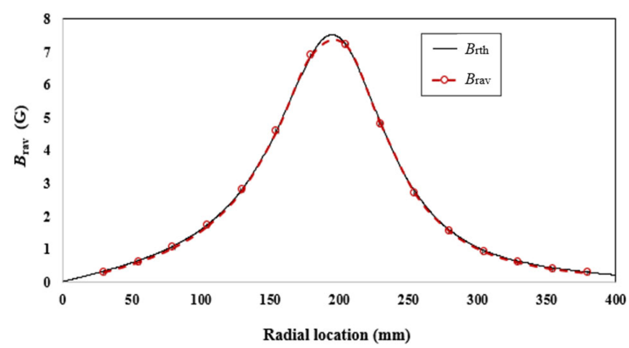

Fig. 10 (Color online) Theoretical curve and measured curve

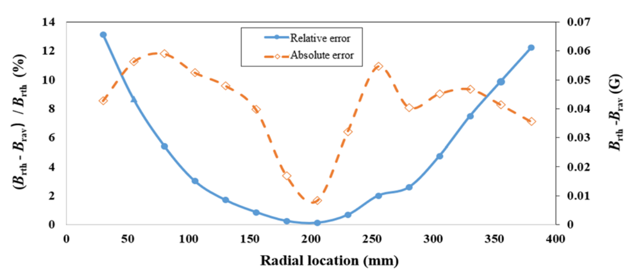

Fig. 11 (Color online) Relative error of the search coil

5 Conclusion

In summary, this paper presents the detailed design and commissioning for a B_{rav} measurement system. The commissioning platform was designed to verify the measurement precision based on the electromagnetic induction principle. Under the testing magnetic field, the coil speed of 2.5 mm/s is considered to be the optimal speed for the search coil. The relative error was approximately 0.1% under the maximum B_r of 7 G. The measurement precision reached 1.0×10^{-3}, which satisfies the measurement requirements.

The analysis and results are of great significance for the B_r measurement of the SC200 proton therapy superconducting cyclotron. However, the measurement error of the system exceeds 10% in edge radius ranges; thus, in the future, we must improve the measurement precision by optimizing the system structure or researching a reasonable optimization method.

References

1. G.A. Karamysheva, O.V. Karamyshev, N.A. Morozov et al., Magnetic system for SC200 superconducting cyclotron for proton therapy, in *Proceedings of Cyclotrons 2016, Zurich, Switzerland, Cyclotrons* (2016), pp. 353–355. https://doi.org/10.18429/jacow-cyclotrons2016-thc03
2. M.M. Xu, Y.T. Song, Conceptual design of scanning magnets for superconducting proton therapy facility. IEEE Trans. Appl. Supercond. **27**, 1–8 (2017). https://doi.org/10.1109/TASC.2017.2698201
3. J.I.M. Botman, H.L. Hagedoorn, Median plane effects in the Eindhoven AVF cyclotron. IEEE Trans. Nucl. Sci. **28**, 2128–2130 (1981). https://doi.org/10.1109/TNS.1981.4331613
4. S. Brandenburg, W.K. van Asselt, M.A. Hofstee, et al., Vertical beam motion in the AGOR cyclotron, in *Proceedings of EPAC 2004, Switzerland* (2004), pp. 1384–1386. http://accelconf.web.cern.ch/AccelConf/e04/PAPERS/TUPLT098.PDF. Accessed 20 Mar 2018
5. J. Stursa, V. Bejeovec, A. Borkovzi et al., The axial injection system of the isochronous cyclotron (1992), pp. 1513–1515. http://accelconf.web.cern.ch/AccelConf/e92/PDF/EPAC1992_1513.PDF. Accessed 20 Mar 2018
6. S. Vorojtsov, N. Morozov, E. Bakewicz et al., Harmonic coil application for shaping of the magnetic field of isochronous cyclotron AIC-144, (2000). http://www.jinr.ru/Preprints/2000/P9200039.pdf. Accessed 20 Mar 2018
7. J. Van de Walle, W. Kleeven, C. L'Abbate, et al. Mapping of the new IBA superconducting SYNCHROCYCLOTRON (S2C2) for proton therapy, in *Proceedings of Cyclotrons, Vancouver, BC, Canada* (2013), pp. 272–274. http://accelconf.web.cern.ch/AccelConf/CYCLOTRONS2013/papers/tu4pb01.pdf. Accessed 20 Mar 2018
8. K.H. Park, Y.G. Jung, D.E. Kim et al., Field mapping system for cyclotron magnet. Nucl. Inst. Methods Phys. Res. A **545**, 533–541 (2005). https://doi.org/10.1016/j.nima.2005.02.009
9. S. Marks, Precise integration of undulator Hall probe scans. IEEE Trans. Magn. Mag. **30**, 2435–2438 (1994). https://doi.org/10.1109/20.305769
10. Y. Paradis, D. Vandeplassche, W. Beeckman, et al. The magnetic field mapping system for the IBA C70 cyclotron. Cyclotr. Appl. (2007). http://accelconf.web.cern.ch/accelconf/c07/PAPERS/78.PDF. Accessed 20 Mar 2018
11. A. K. Jain, *Overview of magnetic measurement techniques*. CERN Academic Training Program (2003). http://cds.cern.ch/record/610089. Accessed 20 Mar 2018
12. M. Li, Y.L. Lv, L. Cao et al., Field mapping system design for the superconducting cyclotron CYCIAE-230. IEEE Trans. Appl. Supercond. **28**, 1 (2018). https://doi.org/10.1109/TASC.2018.2789447
13. A. K. Jain, *Magnetic field measurements and mapping techniques*. CERN Academic Training Program (2003). http://cds.cern.ch/record/610089?ln=zh_CN. Accessed 20 Mar 2018
14. K.N. Henrichsen, Classification of magnetic measurement methods. CERN **16**, 70–83 (1992). https://doi.org/10.5170/CERN-1992-005.70
15. L.H. Harwood, J.A. Nolen, M. Fowler et al., Characteristics and performance of the system developed for magnetic mapping of the NSCL superconducting K800 cyclotron magnet. IEEE Trans. Nucl. Sci. **32**, 3734 (1985). https://doi.org/10.1109/tns.1985.4334485
16. G.A. Karamysheva, S.G. Kostromin, N.A. Morozov, et al., Development of a method for measuring the radial component of the magnetic field in AVF cyclotrons, in *Accelerator Technology Main Systems: Proceedings of IPAC2014* (2014), pp. 1274–1276. https://doi.org/10.18429/jacow-IPAC2014-TUPRO099
17. G. Karamysheva, N. Morozov, P. Shishlyannikov, Median plane effects and measurement method for radial component of magnetic field in AVF cyclotrons, in *Magnet and Vacuum: Proceedings of CYCLOTRONS 2010, Lanzhou, China*, Cyclotrons (2010), pp. 206–208. https://doi.org/10.18429/jacow-APAC2010-MOPCP077
18. A. Roy, T. Bhattacharjee, R.B. Bhole, et al., Median plane magnetic field mapping for superconducting cyclotron (SCC) in VECC, in *Accelerator Technology: APAC 2007, Raja Ramanna Centre for Advanced Technology (RRCAT), Indore, India* (2007), pp. 652–654. https://doi.org/10.18429/jacow-APAC2007-THPMA016
19. O.V. Karamyshev, G.A. Karamysheva, N.A. Morozov, et al., Beam tracking simulation for SC200 superconducting cyclotron (2016), pp. 1268–1271. https://doi.org/10.18429/jacow-ipac2016-tupmr018
20. N.A. Morozov, O.V. Karamyshev, G.A. Karamysheva, et al., Computer modeling of magnet for SC200 superconducting cyclotron, in *Hadron Accelerators: Proceedings of IPAC2016, Busan, Korea, Cyclotrons* (2016), pp. 1265–1268. https://doi.org/10.18429/jacow-ipac2016-tupmr017
21. K.Z. Ding, Y.F. Bi, G. Chen, et al., Study of the beam extraction from superconducting cyclotron SC200, in *Proceedings of Cyclotrons2016, Zurich, Switzerland, Cyclotrons* (2016), pp. 87–91. https://doi.org/10.18429/jacow-cyclotrons2016-mop14
22. G.A. Karamysheva, Y.F. Bi, G. Chen, et al., Compact superconducting cyclotron SC200 for proton therapy, in *Proceedings of Cyclotrons2016, Zurich, Switzerland, Cyclotrons* (2016), pp. 371–373. https://doi.org/10.18429/jacow-cyclotrons2016-thc03